Molecular variation of capillary-produced soft x-ray high harmonics

2008 J. Phys. B: At. Mol. Opt. Phys. 41 145602

(http://iopscience.iop.org/0953-4075/41/14/145602)

J. Phys. B: At. Mol. Opt. Phys. **41** (2008) 145602 (8pp) doi:10.1088/0953-4075/41/14/145602

Molecular variation of capillary-produced soft x-ray high harmonics

S L Stebbings[1], E T F Rogers[2], A M de Paula[1,4], M Praeger[1], C A Froud[2,5], B Mills[2], D C Hanna[2], J J Baumberg[1,6], W S Brocklesby[2] and J G Frey[3]

[1] School of Physics and Astronomy, University of Southampton, Southampton SO17 1BJ, UK
[2] Optoelectronics Research Centre, University of Southampton, Southampton SO17 1BJ, UK
[3] School of Chemistry, University of Southampton, Southampton SO17 1BJ, UK

E-mail: slw3@soton.ac.uk

Received 10 April 2008, in final form 23 May 2008
Published 4 July 2008
Online at stacks.iop.org/JPhysB/41/145602

Abstract
The production of coherent soft x-rays via high harmonic generation (HHG) from Ar, N_2 and N_2O in a gas-filled capillary waveguide is reported. Odd harmonics of the driving laser intensity are observed as a function of gas pressure up to energies of 50 eV. By employing a simple phase matching theory that incorporates the spatial and temporal dependences of ionization within the waveguide, good agreement with the HHG spectral envelope has been obtained, indicating phase matching is the dominant factor in shaping the spectral envelope of the harmonics.

(Some figures in this article are in colour only in the electronic version)

1. Introduction

The nonlinear response of atoms and molecules exposed to an ultrafast, high-intensity laser field can be used to produce coherent, sub-femtosecond soft x-ray pulses via the high harmonic generation (HHG) process.

The HHG process is most commonly understood as a semi-classical three-step model [1–3]. Initially the combination of the laser field with the atomic potential increases the tunnelling probability of part of the valence electron wavefunction through the modified potential barrier into the continuum during the first half-cycle of the laser field. The laser field accelerates the liberated electron wavefunction, and in the case of a linearly polarized laser field, the electron will be driven back to its parent ion when the laser field reverses. Depending upon the phase at which the electron was ionized, it can subsequently recombine with its parent ion. An oscillating electric dipole is created when the fraction of the electron wavefunction which has been accelerated interferes with the fraction which has remained in the atom core and this oscillating dipole can emit in the soft x-ray. Harmonics are created as this process is repeated every half-cycle of the laser pulse.

HHG has been investigated in three experimental configurations: gas cells [4–6], capillary waveguides [7–9], gas jets [10–12] as well as combined capillary and jet geometries [13]. Factors such as the propagation geometry, peak laser intensity and properties of the generating gas all have significant influence on the efficiency of soft x-ray production. Manipulating these parameters to improve phase matching between the fundamental laser and harmonic fields (i.e. minimizing their phase mismatch, Δk) can lead to a significant enhancement in the x-ray output [14–17].

The laser propagation geometry employed has a significant effect on the phase matching of the high harmonics produced. While the gas jet geometry exploits the Guoy phase shift for efficient generation, the capillary waveguide in principle gives an extended interaction length between the laser and the gas medium. The resulting x-ray harmonic spectrum is profoundly affected by the amount of ionization within the capillary, because of both its effect on the propagating laser [18] and its effect on phase matching via the refractive index of the plasma created.

[4] Present address: Departamento de Física-ICEX, Universidade Federal de Minas Gerais, Caixa Postal 702, 30123-970 Belo Horizonte-MG, Brazil.
[5] Present address: Central Laser Facility, Science and Technology Facilities Council, Rutherford Appleton Laboratory, Harwell Science and Innovation Campus, Didcot, Oxfordshire OX11 0QX, UK.
[6] Present address: Department of Physics, University of Cambridge, J J Thompson Avenue, Cambridge CB3 0HE, UK.

In order to effectively test the various theoretical models of HHG, it is essential to investigate as wide a range of targets as possible. To date the majority of such experiments have been limited to the noble gases, with limited number employing molecular gases such as N_2, O_2 and CO_2 [19–21] in a gas jet geometry. This current work extends upon previous observations to study the harmonic emission in a capillary waveguide from three gases of increasing complexity: atomic Ar and the linear diatomic and triatomic molecules of N_2 and N_2O respectively. The soft x-ray spectra are measured as a function of gas pressure, and the spectral envelope of the harmonics is compared to the envelope predicted by solely considering the effects of phase matching.

It is significant and perhaps surprising that the phase matching model describes the spectral envelope of the harmonics, and the maximum energy of the highest order harmonic so effectively without the need to invoke atomic quantum mechanical simulations [22]. Under our experimental conditions, 56 eV is the highest energy harmonic we expect to see for argon according to the cut-off law, given by $E_{\max} = h\nu = I_p + 3.17$ where I_p and U_p are the ionization and ponderomotive potentials respectively. This is higher than the experimentally observed cut-off. As a result harmonic generation occurs in the plateau region and therefore phase-matching effects dominate the spectral envelope, rather than single-atom effects.

The paper is structured as follows—the theoretical calculations are described in section 2, with the experimental configuration and parameters in section 3. The theory is then applied and compared to the experimental HHG spectra from Ar, N_2 and N_2O in section 4. Following a discussion of the results, the conclusions are presented in section 5.

2. Spatio-temporal phase matching

An initial model of the effect of phase matching on HHG in a capillary waveguide was proposed by Durfee *et al* [23]. In this theory, the radial variation of ionization across the capillary mode was included in the propagation via modal averaging, but the possibility of varying phase matching conditions across the capillary was not considered. Extending from the original theory, our current work allows for both the temporal and spatial dependence of the ionization within the capillary, necessary because the Rayleigh length for the soft x-ray output is long, and over the short length of the interaction here the soft x-ray output at different radii do not necessarily interfere—thus different phase matching criteria exist not only at different times, as noted in [23], but also at different positions across the mode. In order to calculate the ionization distribution, the laser intensity is calculated as a function of both radius and time using the capillary modes described by Marcatili [24] and assuming that only the lowest order EH_{11} mode is present. The pulse temporal profile is assumed to be Gaussian. Ionization levels varying in time through the pulse and radially in space are calculated using the ADK tunnelling theory [25, 26]. The calculated ionization fraction is used to calculate the phase mismatch, Δk, between the laser field propagating in the EH_{11} capillary mode and the generated harmonic fields given (in SI units) by

$$\Delta k \approx \frac{q u_{ij} \lambda_0}{4\pi a^2} + N_e r_e (q\lambda_0 - \lambda_q) - \frac{2\pi N_{\text{atm}} P}{\lambda_q}(\delta(\lambda_0) - \delta(\lambda_q)), \quad (1)$$

where q is the harmonic order, u_{ij} is the jth root of the Bessel function, J_{i-1}, where i and j denote the mode (in this case both i and j equal 1 for the EH_{11} capillary mode), λ_0 and λ_q are the wavelengths of the laser and harmonic order q respectively, a is the capillary radius, N_e is the number of electrons, r_e is the classical radius of the electron, N_{atm} is the number of atoms, P is the gas pressure, $\delta(\lambda_0)$ and $\delta(\lambda_q)$ are the dispersion of the neutral gas at the laser and harmonic wavelengths respectively. To reconstruct the space- and time-dependent intensity of the qth order harmonic $I(r, q, t)$ as a function of gas pressure, P, the phase mismatch, Δk, calculated previously is substituted into the equation:

$$I(r, t, q) \propto \mathrm{d}N \left(\frac{1 + \mathrm{e}^{-\alpha L} - 2\,\mathrm{e}^{-\alpha L} \cos \Delta k L}{\alpha^2 + \Delta k^2} \right), \quad (2)$$

where $\mathrm{d}N$ is the number of ions produced in a given time interval, α is the field attenuation coefficient, L is the length of the capillary and $I(r, q, t)$ is the space- and time-dependent intensity of the qth order harmonic. It should be noted that both equations (1) and (2) are modified from those in Durfee *et al* [23] to allow for the spatio-temporal phase matching of the current work. The validity of this calculation depends on the fact that the capillary waveguide is so large on the scale of the soft x-ray wavelength that the generated soft x-ray propagates with the capillary as a plane wave, rather than as a capillary mode. In addition, the intrinsic phase of the generated soft x-ray, due to the phase accumulated between tunnelling and recombination [27], is assumed not to vary across the capillary, i.e. to be independent of intensity. This is a good approximation only for the shorter of the two possible trajectories the electron can travel to emit at a particular wavelength.

Figure 1 shows the result of the spatially and temporally varying phase matching calculations described previously. Each spatial and temporal region phase matches differently as it propagates through the capillary, allowing the calculation of the expected total soft x-ray output due to phase matching summed over all harmonic orders for Ar, N_2 and N_2O, at a pressure of 50 mbar. No single-atom effects are included in this calculation beyond a simple cut-off at $h\nu = I_p + 3.17\,U_p$. The figures show contours of laser intensity as a function of time and radial position within the pulse, and the total soft x-ray output is shown as a greyscale variation.

Figure 1(a) illustrates the implications of this calculation for generation in Ar. Phase matched build up of soft x-ray is predicted for laser intensities ranging from 1.6 to 1.8 $\times$ 10^{14} W cm^{-2}. On the capillary central axis ($r = 0$), little phase matched build up of soft x-ray is predicted on the rising edge of the pulse at times before -5 fs, as insufficient Ar atoms have been ionized for phase matching to occur within this region. At times later than approximately 1 fs, no phase matched build up is seen on-axis because the ionization level

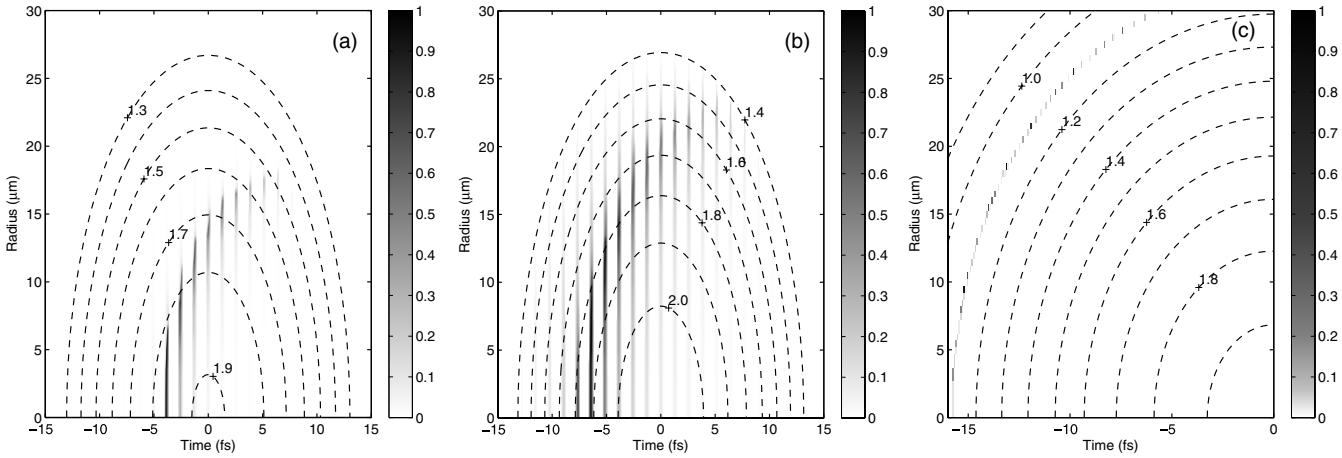

Figure 1. Theoretical harmonic intensity distribution, $I(r, t)$ summed over all harmonic orders q and plotted as a function of (r, t) for (a) Ar, (b) N_2 and (c) N_2O. The maximum signal has been normalized to 1. Also shown are the iso-intensity contours of the applied laser intensity multiplied by 10^{14} W cm^{-2}.

of the Ar is too high. However, phase matching is effective at times later than 1 fs at larger radii, as the intensity is lower. Later in the pulse, effective phase matching becomes increasingly weighted towards larger radii. No harmonics are expected for intensities greater than 1.9×10^{14} W cm^{-2} due to the high ionization fraction, or at intensities less than 1.5×10^{14} W cm^{-2} where the laser intensity is insufficient to drive the tunnelling process.

Similar trends are observed when N_2 is used as the target gas, figure 1(b). Once again the soft x-ray signal is increasingly weighted towards larger radii as the ionization fraction increases with time. However in contrast to Ar, a significant amount of the harmonic signal is predicted much earlier in the pulse (from $t = -7.5$ fs). Furthermore, phase matched soft x-ray generation is also expected out to $r \approx 23$ μm where the laser intensity is 1.4×10^{14} W cm^{-2}. These observations are consistent with the lower ionization potential of N_2 leading to a higher ionization fraction earlier in the laser pulse and causing effective phase matching further out from the capillary core.

The differences between Ar and N_2 are minor when compared to N_2O, figure 1(c). Here the predicted harmonic signal is highly localized in both r and t for laser intensities between 1 and 1.2×10^{14} W cm^{-2}. This suggests only a small fraction of the laser intensity will provide optimal phase matching conditions for high harmonic generation. This is explained in part by the ionization properties of N_2O, which are significantly different from those of Ar and N_2. Other properties such as the plasma index and the amount of neutral gas also have a significant effect on the harmonic build up. It is predicted that the radially dependent phase matching build up of HHG will lead to a structured x-ray beam both temporally and spatially [7], also leading to spectro-spatial coupling. In the far field, spectro-spatial coupling will remain, although the simple radial form here will be altered by propagation after leaving the capillary.

In the current work the spectra of the x-ray beam have been measured as a function of gas pressure and type i.e. Ar, N_2 and N_2O. By calculating the phase matched build up with respect to r and t, the theoretical envelope of individual harmonic orders, q, can be generated to compare with experiment. In this comparison, however, it is important to note that only the build up of soft x-ray intensity controlled by phase matching is calculated. The only single atom effect included in the modelling is the spatially and temporally dependent cut-off energy, $E_{\max}$, which is given by $I_p + 3.17\,U_p$.

Harmonic envelopes are calculated using a typical peak intensity of 2×10^{14} W cm^{-2} measured at the exit of the capillary, using the spatially dependent theory of the current work for Ar, N_2 and N_2O over a wide range of gas pressures. These are then compared with the experimental data and discussed in section 4.

3. Experimental configuration

A schematic of the experimental configuration employed in the current work is shown in figure 2.

A Ti:Sapphire chirped pulse amplification system is used to provide pulses of 35 fs duration and 1 mJ energy at a central wavelength of 780 nm and 1 kHz repetition rate. The pulses are then focused into a hollow fused silica capillary waveguide of 7 cm length and inner diameter of 150 μm, to give a peak intensity of approximately 2×10^{14} W cm^{-2} at the exit. A pair of 300 μm diameter holes were drilled 2 cm from either end of the capillary which allow gas from a pressure regulated supply to be fed into the capillary defining a central region of constant pressure. As both the laser and generated x-ray beams are collinear, a 200 nm thick aluminium filter is employed to block the laser while allowing approximately 10% of the x-rays to be transmitted. The x-ray beam is spectrally dispersed with a grazing incidence spectrometer and detected using a multi-channel plate and CCD. The pressure within the capillary can be varied from 5 to 200 mbar. In the current work the high harmonic spectra of Ar, N_2 and N_2O are recorded as a function of gas pressure from 10 to 110 mbar. These results are compared with both spatially independent and dependent calculations in the following section.

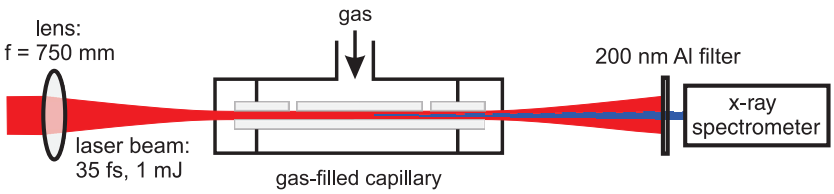

Figure 2. Schematic of the experimental set-up employed in the current work. The gas pressure is regulated by a computer-controlled valve and is fed into the capillary via two 300 μm diameter micro-machined holes.

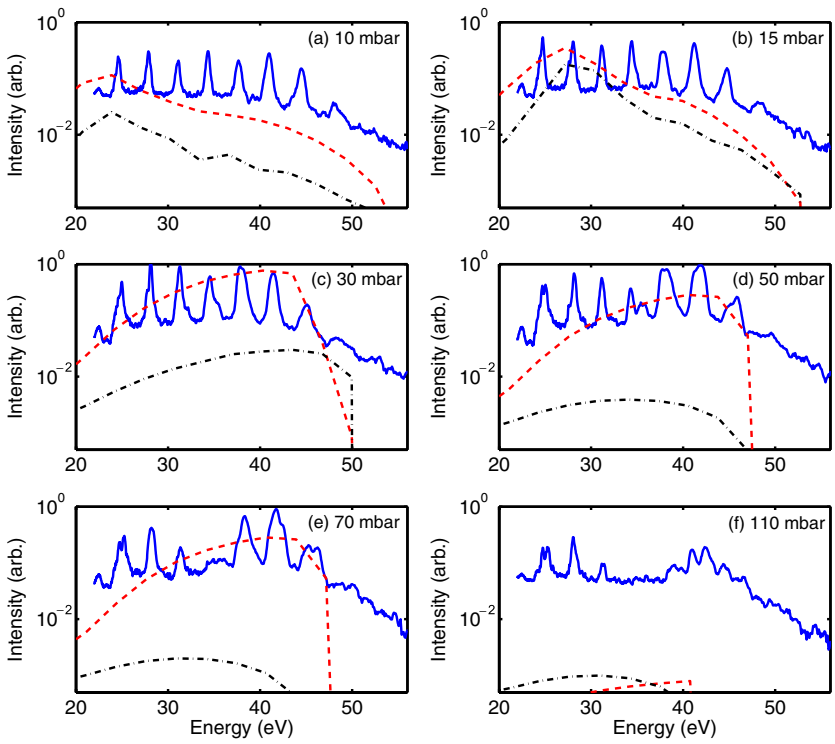

Figure 3. High harmonic generation from Ar as a function of gas pressure. The measured high harmonic spectra (solid blue line) are modelled using the spatially independent (back dash-dotted line) and dependent (red dashed line) phase matching theories.

4. Results and discussion

The high harmonic spectra generated from Ar for six different pressures 10–110 mbar are presented in figure 3. The transmission of the high harmonics through the 200 nm aluminium filter and two layers of aluminium oxide have been allowed for in all of the experimental data presented in this work.

The experimental data are compared with the spectral envelopes using the spatially dependent phase matching calculations. Also included for completeness are spectral envelopes calculated without including spatial variation of the ionization levels. Both the data and theoretical curves are scaled correctly between different pressures–the experimental data can be compared directly between pressures, and the theoretical curves can also be similarly compared. The overall scaling of the predicted soft x-ray output from phase matching is performed at a single pressure, where the maximum predicted signal is obtained, and applied to all other pressures, as the calculation cannot give absolute soft x-ray intensities. Thus the decrease in output seen in both the theory and experiment between, for example, 30 mbar and 10 mbar, are real for both data and calculation.

Below ≈50 mbar, the Ar spectral data show seven well-defined harmonic peaks of near uniform intensity, with a small peak at the highest observed energy, across an energy range from 25 to 50 eV. Comparison of experimental data (solid line) and the spatially dependent theoretical envelopes (dashed line) below pressures of ≈70 mbar are reasonable, giving prediction of the shape of the envelope, relative intensity between pressures, and the highest observed harmonics (the 'cut-off' predicted using the semi-classical formula I_p + 3.17 U_p is ≈56 eV for these data, higher than any harmonic observed). The spatially-independent calculations (dot-dash line) are significantly less effective at predicting both the envelope shape, relative intensity between pressures and highest observable harmonic.

As the gas pressure within the capillary is increased above ≈50 mbar, the spectra show clear indications that more complex effects are starting to occur. At 70 mbar the harmonics are no longer narrow and single-peaked, and at 110 mbar the high-energy harmonics have merged to form a

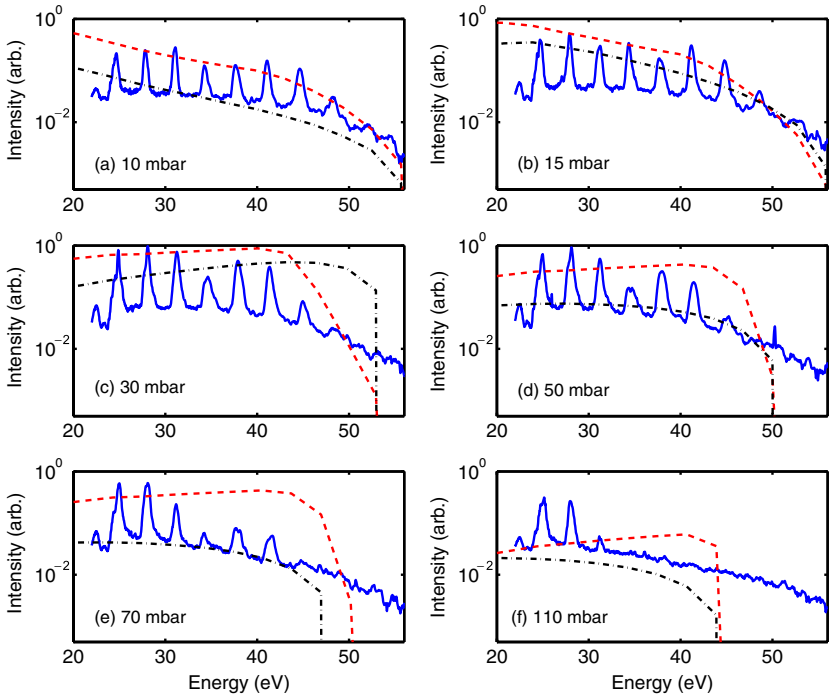

Figure 4. High harmonic generation from N_2 as a function of gas pressure. The measured high harmonic spectra (solid blue line) are modelled using the spatially independent (back dash-dotted line) and dependent (red dashed line) phase matching theories.

continuum, with complex structure developing on the peaks below 32 eV. The peak at 35 eV gradually splits and broadens with pressure, almost disappearing at 110 mbar. The simple phase matching calculations here are obviously unable to reproduce this behaviour. The envelope is well reproduced by calculation up to 70 mbar, but at 110 mbar the calculation does not reproduce the observed data. It is known that at higher pressures, propagation of the driving laser pulse in highly-ionized gas causes significant pulse distortions, with blue shifting, broadening [18] and temporal compression [28] having been previously observed. This is likely to be the source of the distortion in the harmonic spectrum, and any variation in the propagation of the pulse will nullify the phase matching calculations.

High harmonic generation from N_2 was also studied as a function of gas pressure, with the results presented in figure 4. For low pressures of 10 and 15 mbar, figures 4(a) and (b) respectively, the spectra display eight well-defined peaks ranging in energy from 25 to 50 eV, with near identical intensity distribution to those produced from Ar at the same pressures which can be explained by the similarity in the ionization potentials of these two gases (15.58 and 15.76 eV respectively). The spectral envelopes produced by spatially-dependent phase matching calculations again display good agreement with the experimental data up to pressures of ≈50 mbar. As the pressure is increased above 50 mbar, the measured harmonic spectrum from N_2 does not display the same variation of the harmonic lineshape or intensities observed from Ar. Instead the harmonic intensities remain more evenly distributed with the most intense harmonics observed from 25 to 30 eV. The significant splitting and broadening of the harmonics shown in Ar is not reproduced here and the spectral lines remain reasonably narrow up to high pressures. The slightly lower degree of ionization predicted from simple theory for N_2 may be responsible for this less altered spectrum. The spectrum of the laser transmitted through the capillary at the highest pressure shows less broadening in the case of N_2 than Ar [29], giving experimental backing to this interpretation. The phase matching calculations of the harmonic envelope start to diverge from the data at higher pressures, just as they do in the case of Ar, further indication that other effects are undermining the simple calculation.

In addition to Ar and N_2, high harmonic generation from N_2O was also investigated as a function of pressure, as shown in figure 5. Compared to the harmonic spectra produced from N_2O with those from Ar and N_2, fewer and lower-energy harmonics are observed at all pressures. As pressure is increased within the capillary, the high-energy harmonic peaks are reduced, leaving a much-reduced spectrum at 110 mbar.

Envelopes calculated using phase matching for the harmonics of N_2O do not predict the observed spectral behaviour. The phase matching calculation is very sensitive to the level of ionization present through the pulse, and the calculation of ionization of N_2O is not as accurate as those for Ar and N_2, as the ADK theory is known to be less applicable to a triatomic molecule.

The differences in the measured high harmonic spectra between N_2O and Ar and N_2 are attributed principally to the ionization properties of N_2O, which are significantly different from those for Ar and N_2—the ionization potential of N_2O is 12.39 eV compared to 15.76 and 15.58 eV of Ar and N_2 respectively. As discussed previously, absorption and the

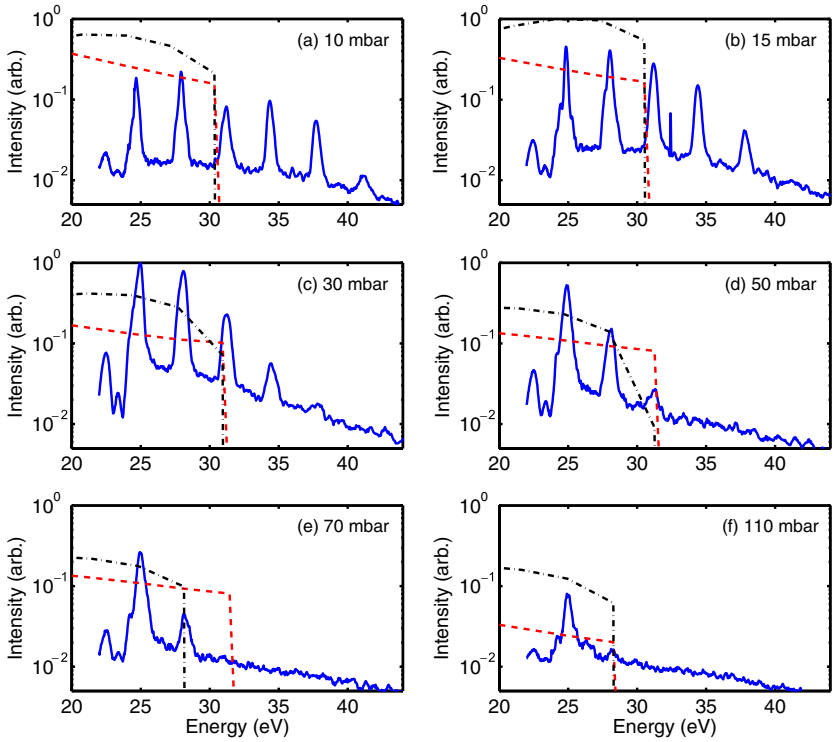

Figure 5. High harmonic generation from N_2O as a function of gas pressure. The measured high harmonic spectra (solid blue line) are modelled using the spatially independent (back dash-dotted line) and dependent (red dashed line) phase matching theories.

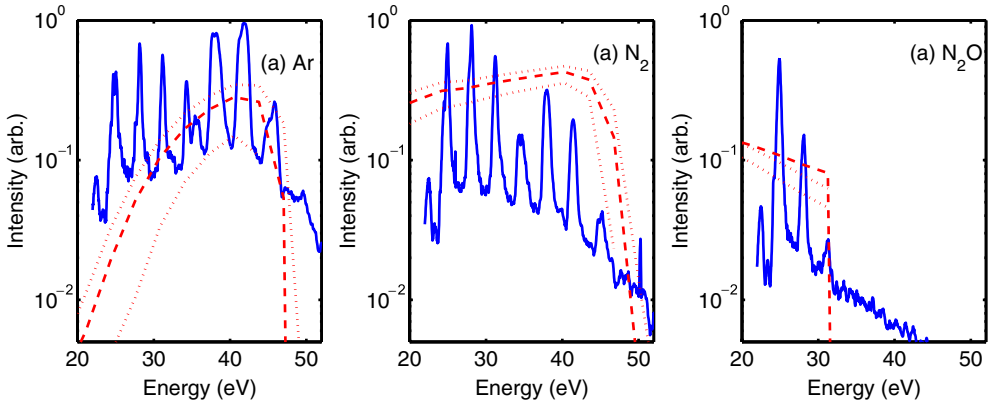

Figure 6. High harmonic spectra of Ar, N_2 and N_2O at 50 mbar (blue solid line). The theoretical harmonic envelopes are shown for peak laser intensities of 2×10^{14} W cm^{-2} (red dashed line), 1.8×10^{14} W cm^{-2} and 2.2×10^{14} W cm^{-2} (red dotted lines).

amount of neutral gas will also affect the measured harmonic signal. The radial dependence of HHG in a capillary leads to a spectrally, spatially and temporally structured x-ray pulse. Further studies of the spatio-temporal variations of the x-ray pulse will give more information.

For a system producing harmonics under ideal phase matching conditions, not subject to absorption by the generating gas, the cut-off energy, $E_{max} = I_p + 3.17\ U_p$. For all three gases, the observed cut-off energy was lower than expected according to this model because of phase matching effects. The calculated and observed cut-off energies, E_{max}, are summarized in table 1.

Table 1. Comparison of the theoretical (using $I_p + 3.17\ U_p$) and observed cut-off energies of the highest order harmonic generated from 30 mbar of N_2O, N_2 and Ar for a peak, on-axis laser intensity of 2×10^{14} W cm^{-2}.

			Cut-off energy (eV)	
Gas	I_p (eV)	I_p +3.17 U_p (eV)	Theory	Experimental
N_2O	12.39	53	31	34
N_2	15.58	56.2	50	50
Ar	15.76	56.3	50	50

In calculating the cut-off energy using $I_p + 3.17\ U_p$, the intensity of 2×10^{14} W cm^{-2} at the exit of the capillary

was used. This is because we assume we are limited to detecting those harmonics produced within the final few mm of the waveguide due to the absorption of the generating gas. Experimentally the maximum observed photon energy is limited by the absorption of the generating gas as well as phase matching effects. Only by employing the spatially dependent phase matching calculations can the experimental cut-off energies be consistently reproduced by the theory. These observations highlight the importance of including spatially dependent ionization within the theory for capillary-based high harmonic generation.

In order to determine how robust the spatially dependent theory is, the driving laser intensity was varied within the measured experimental error of $\pm 10\%$ and fed into the calculations. The resulting harmonic envelopes are compared to the experimental data of Ar, N_2 and N_2O for a pressure of 50 mbar in figure 6. It is clear that a 10% intensity variation has no significant effect on the overall shape of the envelope.

This procedure was repeated in order to investigate the effects of the gas pressure variation on the harmonic envelope generated by the theory. It is estimated that the measured pressure within the capillary waveguide has an error of ± 2 mbar. Theoretical envelopes are generated for Ar, N_2 and N_2O for pressures of 48, 50 and 52 mbar and are compared to the experimental data at 50 mbar. The estimated error in the pressure was found to have no significant effect on either the cut-off energy or the overall shape of the predicted spectral envelope.

5. Conclusions

We have presented and compared the HHG from Ar, N_2 and N_2O in a gas-filled capillary for the first time. By modifying a simple phase matching theory to incorporate spatial and temporal dependences of the HHG process, improved agreement with the experimental data has been achieved without the need for a complex quantum mechanical treatment. While this agreement is most apparent for Ar and N_2, N_2O is less well modelled. The probable reason for this is the atomic tunnelling theory used to determine the ionization fraction in N_2O. Clearly an improvement would be to develop a more rigorous technique for determining the ionization fraction in a triatomic molecule.

It is further observed that the effect of spatial and temporal HHG within a gas-filled capillary waveguide only become significant for pressures in excess of 15 mbar for all three gases investigated. Below this pressure both spatially independent and dependent phase matching calculations predict similar cut-off energies and harmonic envelopes. At low pressures the number density of the ions off-axis is negligibly small, thus decreasing the effect of any spatially dependent HHG. Agreement between the theory and experimental data at 110 mbar is less convincing due to temporal distortions in the driving laser pulse as it propagates through the target gas. Consequently, an improvement would be to incorporate a pressure dependence into the laser pulse profile.

This work clearly shows incorporating spatial effects into theoretical calculations of capillary HHG is necessary for modelling experimental observations. Accurate models with spatial and temporal dependences will allow optimal conditions for capillary HHG to be determined; this will be of particular value in quasi-phase matching experiments.

Acknowledgments

This work is supported by Research Councils UK Basic Technologies Programme. EPSRC studentships are gratefully acknowledged by ETFR, BM and CAF. MP acknowledges support from the Basic Technologies Programme.

References

[1] Corkum P B 1993 *Phys. Rev. Lett.* **71** 1994–8
[2] Lewenstein M, Balcou Ph, Ivanov M Yu, L'Huillier A and Corkum P B 1994 *Phys. Rev.* A **49** 2117–32
[3] Schafer K J, Yang B, DiMauro L F and Kulander K C 1993 *Phys. Rev. Lett.* **70** 1599–602
[4] Sutherland J, Christensen E, Powers N, Rhynard S, Painter J and Peatross J 2004 *Opt. Express* **12** 4430–6
[5] Kazamias S, Douillet D, Weihe F, Valantin C, Rousse A, Sebban S, Grillon G, Augé F, Hulin D and Balcou Ph 2003 *Phys. Rev. Lett.* **90** 193901
[6] Tamaki Y, Itatani J, Nagata Y, Obara M and Midorikawa K 1999 *Phys. Rev. Lett.* **82** 1422–5
[7] Praeger M, de Paula A M, Froud C A, Rogers E T F, Stebbings S L, Brocklesby W S, Baumberg J J, Hanna D C and Frey J G 2007 *Nat. Phys.* **3** 176–9
[8] Pfeiffer T, Kemmer R, Spitzenpfeil R, Walter D, Winterfeldt C, Gerber G and Spielmann C 2005 *Opt. Lett.* **30** 1497–9
[9] Paul A, Gibson E A, Zhang X, Lytle A, Popmintchev T, Zhou X, Murnane M M, Christov I P and Kapteyn H C 2006 *IEEE J. Quantum Electron* **42** 14–26
[10] Paul P M, Toma E S, Berger P, Mullot G, Augé F, Balcou Ph, Muller H G and Agostini P 2001 *Science* **292** 1689–92
[11] Levesque J, Zeidler D, Marangos J P, Corkum P B and Villeneuve D M 2007 *Phys. Rev. Lett.* **98** 183903
[12] Gagnon E, Ranitovic P, Tong X-M, Cocke C L, Murnane M M, Kapteyn H C and Sandhu A S 2007 *Science* **317** 1374–8
[13] Heinrich A, Kornelis W, Anscombe M P, Hauri C P, Schlup P, Biegert J and Keller U 2006 *J. Phys. B: At. Mol. Opt. Phys.* **39** S275–81
[14] Zhang X, Lytle A L, Popmintchev T, Zhou X, Kapteyn H C, Murnane M M and Cohen O 2007 *Nat. Phys.* **3** 270–5
[15] Seres J, Yakovlev V S, Seres E, Streli Ch, Wobrauschek P and Krausz F 2007 *Nat. Phys.* **3** 878–83
[16] Gibson E A *et al* 2003 *Science* **302** 92–8
[17] T Auguste T, Carré B and Salières P 2007 *Phys. Rev.* A **76** 011802
[18] Froud C A, Rogers E T, Hanna D C, Brocklesby W S, Praeger M, de Paula A M, Baumberg J J and Frey J G 2006 *Opt. Lett.* **31** 374–7
[19] Altucci C *et al* 2005 *Phys. Rev.* A **71** 013409
[20] Shan B, Tong X-M, Zhou Z, Chang Z and Lin C D 2002 *Phys. Rev.* A **66** 061401
[21] Marangos J P *et al* 2006 *J. Mod. Opt.* **53** 97–111

[22] L'Huillier A, Schafer K J and Kulander K C 1991 *J. Phys. B: At. Mol. Opt. Phys.* **24** 3315–41
[23] Durfee C G, Rundquist A R, Backus S, Herne C, Murnane M M and Kapteyn H C 1999 *Phys. Rev. Lett.* **83** 2187–90
[24] Marcatili E A J and Schmeltzer R A 1964 *Bell Syst. Tech. J.* **43** 1783–1809
[25] Ammosov M V, Delone N B and Krainov V P 1986 *Sov. Phys.—JETP* **64** 1191–4
[26] Popov V S 2004 *Phys.—Usp.* **47** 855–85
[27] Lindner F, Stremme W, Schätzel M G, Grasbon F, Paulus G G, Walther H, Hartmann R and Strüder L 2003 *Phys. Rev.* A **68** 013814
[28] Zhang X, Lytle A, Popmintchev T, Paul A, Wagner N, Murnane M, Kapteyn H and Christov I P 2005 *Opt. Lett.* **30** 1971–3
[29] Stebbings S L, de Paula A M, Praeger M, Rogers E T F, Froud C A, Mills B, Baumberg J J, Brocklesby W S, Hanna D C and Frey J G 2006 *Photon06 Conf., Manchester, 4–7 September 2006*